

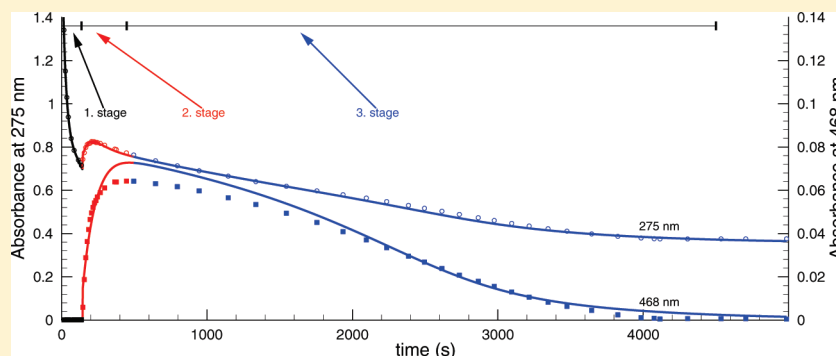
On the Complexity of Kinetics and the Mechanism of the Thiosulfate–Periodate Reaction

Evelin Rauscher, György Csekő, and Attila K. Horváth*

Department of Inorganic Chemistry, University of Pécs, Ifjúság útja 6, H-7624 Pécs, Hungary

S Supporting Information

ABSTRACT:

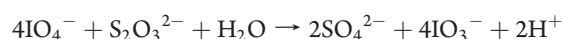


The thiosulfate–periodate reaction has been studied spectrophotometrically in a slightly acidic medium at 25.0 ± 0.1 °C in an acetate/acetic acid buffer by monitoring the absorbance in the 250–600 nm wavelength range at a constant ionic strength adjusted by the buffer component sodium acetate. In agreement with a previous study, we found that the reaction cannot be described by a single stoichiometric equation, tetrathionate and sulfate are simultaneously formed, and its ratio strongly depends on the pH. As expected at certain initial concentration ratios of the reactants, the reaction behaves as a clock reaction, but after its appearance, iodine is slowly consumed mainly because of the moderate tetrathionate–iodine reaction. It is also enlightened that the initial rate of the reaction is completely independent of the pH, which apparently contradicts a previous study, which postulates a “supercatalytic” behavior of the hydrogen ion on the title reaction. Significant buffer assistance that may change the absorbance–time profiles was also observed. On the basis of the kinetic data, a robust 28-step kinetic model with 22 fitted parameters is proposed and discussed to explain adequately all of the important characteristics of the kinetic curves.

INTRODUCTION

Two decades after the 1980s have witnessed the discovery of a rich variety of oscillatory reactions in open systems.^{1,2} By that time, however, only a few chemically different systems were known to oscillate in a batch such as the BZ reaction,^{3,4} the Bray–Liebhafsky reaction,⁵ and the chlorite–iodide–malonic acid reaction.⁶ All of these systems exhibit oscillation at strongly acidic conditions at nearly constant hydrogen ion concentration. The pH is, therefore, adjusted by strong acids (e.g., sulfuric acid, perchloric acid, etc.) in the systems mentioned above. Considerable efforts were devoted in the late 1980s to search such a chemical system that provided pH oscillation in batch. Large-amplitude pH oscillation was found in the closed iodate–sulfite–thiosulfate system by Rábai and Beck.⁷ The phenomenon was explained by the cross-catalytic and inhibitory effects of thiosulfate and sulfite on the sulfite–iodate and thiosulfate–iodate systems, respectively. Later it turned out that a “simple” supercatalytic effect⁸ of the hydrogen ion on the sulfite–iodate reaction and partial regeneration of sulfite in the thiosulfite–iodate reaction was capable of providing a good description of the observed kinetic traces.⁹ Another system reported to exhibit pH

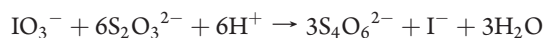
oscillation in closed conditions is the thiosulfate–periodate reaction.¹⁰ It was demonstrated that at certain experimental conditions three extrema appeared in the pH–time curves. Moreover, in a continuously stirred flow reactor (CSTR), sustained and damped oscillations occurred with variation of the initial concentrations of the reactants. The unique feature of this system is that if it is in a steady state temporary perturbation (change of the flow rate, injection of either of the reactants, etc.) results in a rare, fairly long transient period of damped oscillation. Such an unsustained oscillatory behavior in a CSTR is rather uncommon, and by that time, no model has yet been proposed to describe this behavior. Rábai et al. have suggested¹⁰ the simple empirical rate law model



$$v_1 = (k_1[\text{H}^+]^2 + k_1'[\text{H}^+]^3)[\text{IO}_4^-][\text{S}_2\text{O}_3^{2-}] \quad (1)$$

Received: March 28, 2011

Published: May 25, 2011



$$v_2 = k_2[\text{S}_2\text{O}_3^{2-}]^2[\text{IO}_3^-][\text{H}^+]^2 \quad (2)$$

for a qualitative explanation of the phenomena mentioned above. Although it provides a fairly good qualitative agreement, it should be stressed that only the rate term of eq 1 was postulated and no direct kinetic measurements were provided to support this fact. It is, however, not surprising at all that the authors were not able to achieve better agreement because the system is considerably more complicated, and it was even mentioned in their paper that “the system is so complex that we were unable to simulate quantitatively its kinetic behavior”. Here, we, therefore, report our extensive study on the kinetics of the thiosulfate–periodate reaction.

EXPERIMENTAL SECTION

Materials and Buffers. All chemicals were of the highest purity commercially available (acetic acid, sodium acetate, sodium thiosulfate, and potassium metaperiodate) and were used without further purification. Stock solutions were freshly prepared each day from doubly distilled and twice ion-exchanged water. The pH of the solutions was regulated between 4.35 and 5.70 by an acetic acid/acetate buffer, taking the $\text{p}K_a$ of acetic acid as 4.55. The acetate concentration was always kept constant at 0.5 M by controlling an approximately constant ionic strength throughout the experiments, and the pH was adjusted by the necessary amount of acetic acid. The temperature of the reaction vessel was maintained at 25.0 ± 0.1 °C. The concentrations of thiosulfate and periodate were in the ranges 0.5–20.0 and 0.25–4.8 mM, respectively. With this experimental setup, we investigated the reaction at 82 different experimental conditions and we also repeated our experiments in several different cases, which convinced us about the good reproducibility of the kinetic curves (see Figure S1 in the Supporting Information).

Methods and Instrumentation. The reaction was followed by a Zeiss S600 diode-array spectrophotometer. The reaction was carried out in a standard quartz cuvette equipped with magnetic stirrer and a Teflon cap having a 1 cm optical path. The buffer components and periodate were delivered from a pipet first. The spectrum of these solutions was always recorded just before starting the reaction to determine the exact periodate concentration. The reaction was started with the addition of the necessary amount of a thiosulfate solution from a fast-delivery pipet. The spectrum of the reacting solutions at the wavelength range of 250–600 nm was acquired up to approximately 8000 s in every 10 s.

Data Treatment. Matrix rank analysis studies have revealed¹¹ that seven absorbing species exist in the wavelength range of 250–600 nm, namely, the reactants thiosulfate and periodate and the long-lived intermediates and products such as tetrathionate, iodine, triiodide ion, iodate, and iodide ion. Spectra of these species are shown in Figure 1. It is seen that periodate, tetrathionate, and triiodide have strong absorbance bands in the UV range, whereas thiosulfate, iodate, iodine, and iodide have only weak absorption bands. In addition, iodine and triiodide absorb light in the visible range as well. Highly overlapping spectra of the absorbing species prompted us to choose seven different wavelengths for data evaluation to provide enough experimental information about the absorbing species. In the selection of the wavelength, it is considered that the measured absorbance has to be lower than 1.8 because, above this value, the linear relationship between the absorbance and concentration cannot be fulfilled. Therefore, we have chosen the following wavelengths: 275, 280, 285, 290, 350, 400, and 468 nm. Originally, each kinetic run contained more than 700 absorbance–time data pairs at a given wavelength; therefore, it was necessary to reduce the number of

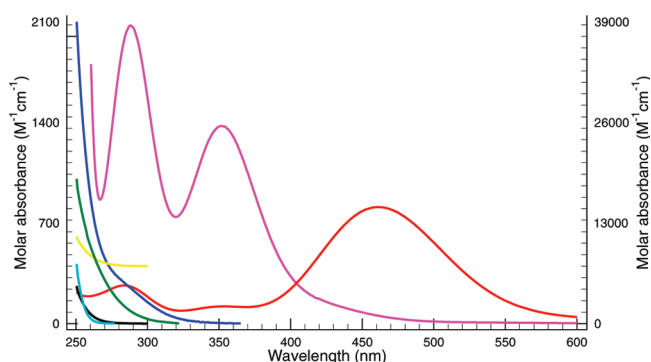
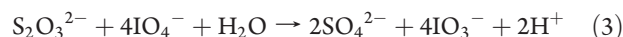


Figure 1. Molar absorbance of the species present in the reaction. The spectra of thiosulfate (black), periodate (blue), tetrathionate (green), iodine (red), iodate (yellow), iodide (cyan), and triiodide (magenta) are indicated by different colors. Note that the right y axis belongs uniquely to the triiodide ion, and the spectrum of iodate (yellow) is shifted along the y axis by $400 \text{ M}^{-1} \text{ cm}^{-1}$ for better visibility.

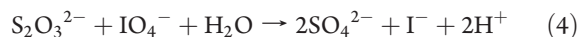
time points (60–70) to avoid unnecessary time-consuming calculations. The essence of this method has already been described elsewhere.¹² To obtain the kinetic model and the rate coefficients, an absolute fitting procedure has been chosen to minimize the average deviation between the measured and calculated absorbance bands. Altogether almost 35 000 experimental points from the 90×7 kinetic series were used for the simultaneous evaluation. Our quantitative criterion for an acceptable fit was that the average deviation for the absolute fit approach 0.006, which is close to the experimentally achievable limit of error under present experimental conditions.

RESULTS

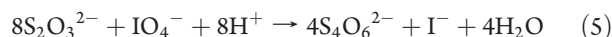
Stoichiometry. The stoichiometry of the reaction was already thoroughly investigated by Rábai et al.¹⁰ It was found that in high excess of periodate the stoichiometry can clearly be characterized by the following equation:



If, however, thiosulfate is in excess, then periodate is reduced to the iodide ion; meanwhile, the tetrathionate and sulfate ions are formed as oxidation products of sulfur according to the following limiting stoichiometric equations:



and



The ratio of eqs 4 and 5 mainly depends on the pH; lower pH prefers the formation of tetrathionate, and the actual stoichiometry at a given experimental condition may be generated by the appropriate linear combination of these equations. Our preliminary investigations clearly confirmed these earlier observations.

Preliminary Observations. The most important characteristics of the measured kinetic curves can be summarized as follows:

Figure 2 shows the effect of the pH on the initial phase of the reaction. As can be seen, a decrease of absorbance in the UV range is independent of the pH, suggesting that the initial step of the reaction does not depend on the pH in the pH range studied. This result is in complete contradiction with the empirical rate

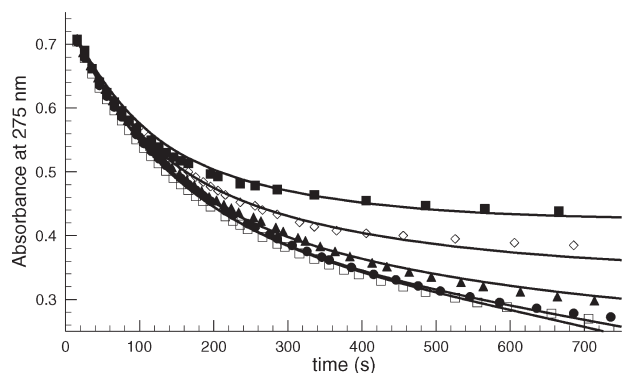


Figure 2. Measured (symbols) and calculated (solid lines) absorbance–time curves at $[\text{S}_2\text{O}_3^{2-}]_0 = 0.5$ mM and $[\text{IO}_4^-]_0 = 2.0$ mM at different pHs: 5.70 (●); 5.55 (□); 5.10 (▲); 4.65 (◇); 4.35 (■).

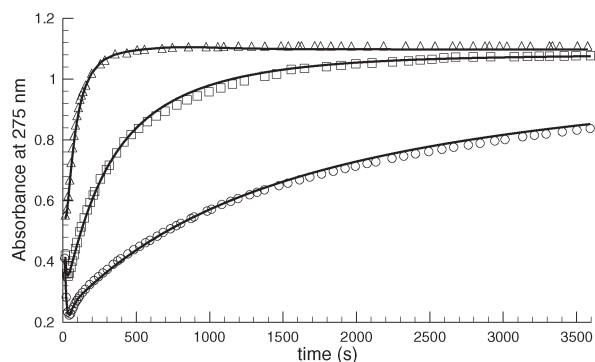


Figure 3. Measured (symbols) and calculated (solid lines) absorbance–time curves at $[\text{S}_2\text{O}_3^{2-}]_0 = 10.0$ mM and $[\text{IO}_4^-]_0 = 2.0$ mM: 5.55 (○); 5.10 (□); 4.65 (△).

law given by Rábai et al., postulating a formal kinetic order of 2 (or even 3) for the hydrogen ion.¹⁰

Figure 3 indicates the shape of the kinetic curves at a 5:1 initial molar ratio of thiosulfate–periodate at different pHs. As can be seen, the absorbance measured in the UV range as a function of time goes through a minimum before leveling off and its minimum value strongly depends on the pH. The lower the pH is, the higher the minimum value of the absorbance becomes. This suggests that eq 5 is preferred over eq 4 at lower pHs because the tetrathionate ion has a strong absorbance band in the UV range.

Figure 4 shows that at certain experimental conditions iodine is formed in a detectable amount, but it reacts further with tetrathionate in a slow reaction,^{13,14} meaning that iodine is a long-lived intermediate of the reaction. This observation is in full accordance with an earlier investigation reported by Rábai et al.¹⁰ It should also be noted that iodine can appear in the solution only if thiosulfate is completely consumed. Therefore, this reaction may also be treated as a Landolt-type reaction,¹⁵ although the sudden appearance of iodine is not so pronounced because of its low concentration in the present case. It is therefore easily conceivable why the Landolt-type behavior of this system has not been discovered yet.

Figure 5 demonstrates the change of shape of the measured absorbance–time series at a constant initial thiosulfate–periodate ratio with increasing thiosulfate concentration. An

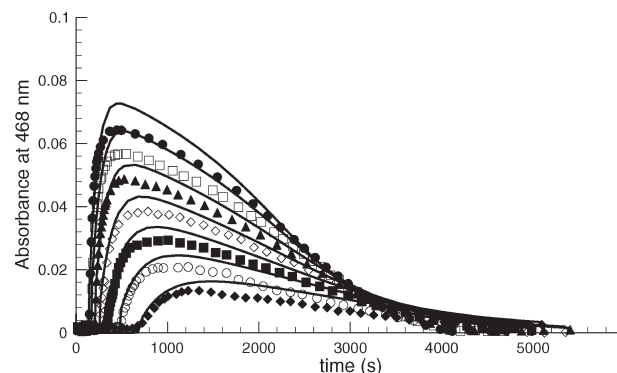


Figure 4. Measured (symbols) and calculated (solid lines) absorbance–time curves at constant $[\text{S}_2\text{O}_3^{2-}]_0/[\text{IO}_4^-]_0 = 4:3$ ratio at pH = 4.65. $[\text{IO}_4^-]_0/\text{mM} = 4.9$ (●), 4.5 (□), 4.0 (▲), 3.5 (◇), 3.0 (■), 2.5 (○), and 2.0 (◆).

increase in the absolute concentration of the reactants results in a more intense rise of the absorbance at 275 nm when thiosulfate is consumed. The maximum in the absorbance is then followed by a slow decrease, which can be attributed to the tetrathionate–iodine reaction.

Figure 6 shows the change of shape of the measured absorbance–time series with varying $[\text{S}_2\text{O}_3^{2-}]_0$ at constant periodate concentration and pH. It is easily seen that a minimum appears in the measured curves as the initial $[\text{S}_2\text{O}_3^{2-}]_0/[\text{IO}_4^-]_0$ ratio increases above 2 and the minimum even becomes lower. It follows from the fact that the ratio of the oxidized sulfur-containing product is shifted toward the formation of tetrathionate over sulfate.

Figure 7 depicts the measured absorbance–time series with changes in the initial periodate concentration at constant low $[\text{S}_2\text{O}_3^{2-}]_0$ and pH. It suggests that under these experimental conditions thiosulfate is mainly oxidized to sulfate.

Initial Rate Studies. The isosbestic point of the iodine–triiodide system seems to be a good candidate for data evaluation of the initial rate because it uniquely refers to the rate of formation of the total amount of iodine ($T_{\text{I}_2} = [\text{I}_2] + [\text{I}_3^-]$). As, however, indicated above (see Figure 4), the reaction behaves as a clock reaction, meaning that iodine can only be observed after a well-defined time lag. Thus, we concluded that the absorbance–time curves measured at the visible range are not appropriate for the initial rate studies. Figure 1 clearly indicates that no wavelength exists in the UV range, where the absorbance can be designated uniquely to one of the absorbing species, but as can be seen, the major absorbing species is periodate. Although triiodide has a very intense absorption band in the UV range, the concentration of this species is basically zero as long as thiosulfate is present in the solution. This means that at the initial phase of the reaction the absorbance change at 275 nm is mainly due to a decrease of the periodate concentration. The molar absorbance of thiosulfate is very small compared to that of periodate and tetrathionate, and therefore a decrease of thiosulfate negligibly contributes to the overall absorbance change. As a result, the net effect at 275 nm is clearly the decrease of absorbance at the beginning stage of the reaction. Thus, we concluded that the absorbance–time series measured at 275 nm is suitable for evaluation of the kinetic curves by the initial rate method. Figure 8 shows the result of the initial rate studies. This clearly indicates that the formal kinetic order of both reactants is 1, but the initial phase of the reaction is

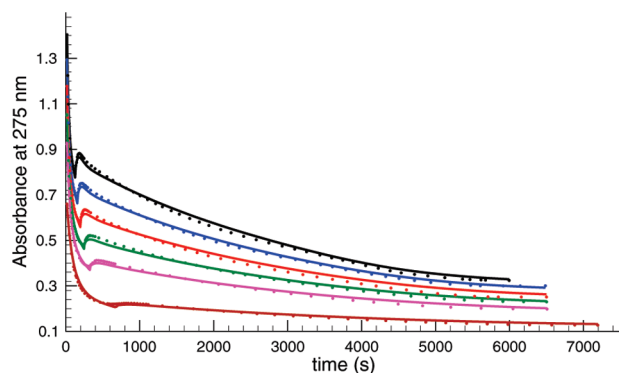


Figure 5. Measured (dots) and calculated (solid lines) absorbance–time curves at a constant $[S_2O_3^{2-}]_0/[IO_4^-]_0 = 1:1.54$ ratio at pH = 4.65. $[IO_4^-]_0/\text{mM} = 5.0$ (black), 4.5 (blue), 4.0 (red), 3.5 (green), 3.0 (magenta), and 2.0 (brown).

completely independent of the pH. One might also argue about the fact that the formation of tetrathionate may disturb the evaluation of the initial rate if its formation strongly depends on the initial concentration ratio of the reactants. More explicitly, there might be a case when although the consumption of periodate increases with decreasing pH at a given time, the shift between eqs 4 and 5 with decreasing pH compensates for the absorbance fall by an increase of the tetrathionate concentration. The net effect may, therefore, be as if the reaction is independent of the pH. It is easily seen that if the apparent unchange of the absorbance–time curves as a function of the pH is a consequence of the latter fact, then a slight pH dependence should occur at different wavelengths just as a result of the difference of the molar absorbance ratio of periodate and tetrathionate. Figure 8, however, indicates that the same formal kinetic order can be obtained for the reactants and the hydrogen ion as well at both wavelengths; therefore, it is confirmed that the initial phase of the reaction is independent of the pH.

Proposed Kinetic Model. The approach we have chosen to analyze our data set has already been successfully applied in several cases of our previous works.^{12,16} The method takes advantage of the significant advances of computing power and resembles the construction of large models such as those in atmospheric¹⁷ and combustion chemistry.¹⁸ The most critical part of this method is to postulate the set of species (reactants, intermediates, and products) involved in the reactions. Besides the reactants (thiosulfate and periodate), the products (tetrathionate, sulfate, iodate, and iodide), and the long-lived intermediates identified by UV–vis spectroscopy (iodine and triiodide), several other intermediates likely to participate in the reaction are postulated such as HSO_3^- , $S_2O_3OH^-$, HIO_2 , HOI , I_2O_2 , $S_2O_3I^-$, and $S_4O_6I^-$. The next step is to find all of the conceivable reactions among all of these species. In the present case, we found 154 different reactions, which are summarized in Table S1 in the Supporting Information. We then considered that all of these reactions have rate equations consisting of three terms: the first one is independent of H^+ , and the second and third ones are proportional to $[H^+]$ and $[H^+]^2$, respectively. This means that we started the fitting procedure with 462 rate coefficients (3×154). As a start, rate coefficients determined from independent studies were fixed and the rest of them were fitted during the evaluation procedure. The rate parameters, which became insensitive for the average deviation between the measured and

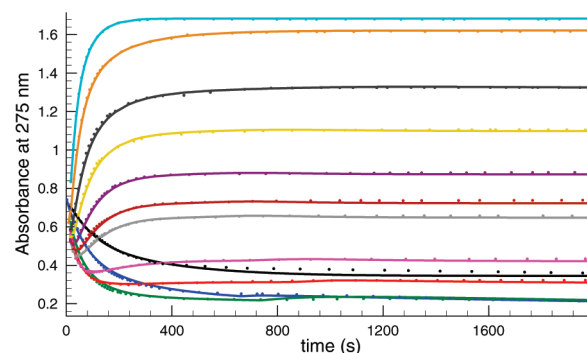


Figure 6. Measured (dots) and calculated (solid lines) absorbance–time curves at a constant $[IO_4^-]_0 = 2.0$ mM ratio at pH = 4.65. $[S_2O_3^{2-}]_0/\text{mM} = 0.5$ (black), 1.0 (blue), 2.0 (green), 3.0 (red), 4.0 (magenta), 6.0 (light gray), 6.66 (brown), 8.0 (purple), 10.0 (yellow), 12.0 (dark gray), 16.0 (orange), and 20.0 (cyan).

calculated data, were omitted step by step, but the omission was only executed if the given parameter became insensitive again after its resensitization. We mean for resensitization that the rate coefficient of the given step was increased to change the value of the average deviation at least by 5%. A slow but straightforward model reduction led us to propose the kinetic model given in Table 1. For the sake of completeness, the molar absorbance of the absorbing species used in the fitting procedure is given in Table 2. The sound agreement between the measured and calculated absorbances at seven different wavelengths (see Figures 2–7 and S2–S7 in the Supporting Information) and the 0.0059 absorbance unit average deviation indicates that the proposed model is working properly within the concentration range used in the experiments.

DISCUSSION

Step 1 is the initiating equilibrium between the reactants that probably proceeds via an O-atom transfer from periodate to thiosulfate to produce iodate and $S_2O_3OH^-$. We found that the forward and reverse reactions are both independent of the pH and their rate coefficients were calculated as $k_1 = 7.36 \pm 0.07 \text{ M}^{-1} \text{ s}^{-1}$ and $k_{-1} = 2.70 \pm 0.03 \text{ M}^{-1} \text{ s}^{-1}$, respectively. It should be emphasized that H^+ is involved only in the stoichiometry of the reactions. Step 1 may therefore be treated as an alternative suggestion for interpreting the sudden rise of the pH at the beginning stage of the reaction observed by Rábai et al. in an unbuffered medium.¹⁰ Separate calculations have shown that pH increases from 5.5 to 5.8 at the initial condition used by Rábai et al. can per se be achieved using step 1 within 2 s, which agrees well with their experimental findings. We should, however, emphasize as well that there is not even a single fact in our experiments indicating any sign of a pH-dependent rate term of the thiosulfate–periodate reaction. Our experiments unambiguously suggest that the pH dependence has to have arisen from the H^+ -dependent pathways of the subsystems of the thiosulfate–periodate reaction. One should also notice that step 1 is an equilibrium, but the stoichiometry and rate laws of the forward and backward reactions are inconsistent with the law of mass action. This discrepancy, however, is only apparent because if one replaces $S_2O_3OH^-$ with $S_2O_4^{2-}$, then the inconsistency disappears. Furthermore, the removal of H^+ can easily be explained by the fast protolytic equilibrium between the species $S_2O_4^{2-}$ and $S_2O_3OH^-$. This argument is also valid in the case of

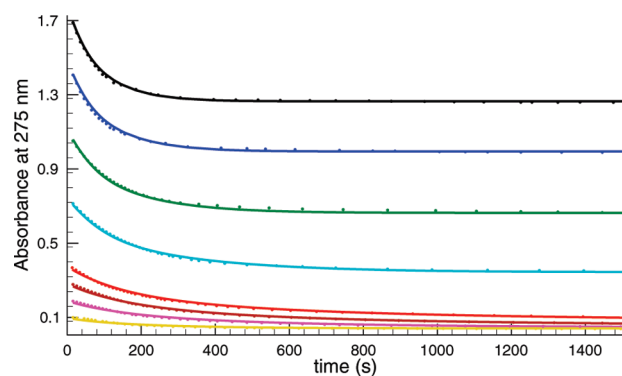


Figure 7. Measured (dots) and calculated (solid lines) absorbance–time curves at a constant $[S_2O_3^{2-}]_0 = 0.5$ mM ratio at pH = 4.65. $[IO_4^-]_0$ /mM = 4.8 (black), 4.0 (blue), 3.0 (green), 2.0 (cyan), 1.0 (red), 0.75 (brown), 0.5 (magenta), and 0.25 (yellow).

step 5 (see later). It should also be noted that periodate exists in four different forms¹⁹ under our experimental conditions such as H_5IO_6 , $H_4IO_6^-$, $H_3IO_6^{2-}$, and IO_4^- , although a more recent study suggests²⁰ the appearance of dimer $H_2I_2O_{10}^{4-}$ in an alkaline solution of periodate whose concentration is negligible at pH = 4.35–5.55. Those species, however, are rapidly equilibrated with each other, and periodate is mainly in a singly charged form (either $H_4IO_6^-$ or IO_4^-) under the present experimental conditions. Because there is a fast equilibrium between these forms and the ratio of $[IO_4^-]/[H_4IO_6^-]$ is 29.5,²¹ it looks reasonable to suppose IO_4^- to be the reactive species despite the fact that our experiments do not provide any solid basis for establishing the kinetically active form of periodate. Thus, in the proposed kinetic model, IO_4^- is supposed in all of those steps in which periodate is involved as a reactant.

Steps 2 and 3 are further oxidations of $S_2O_3OH^-$ by the periodate ion. An interesting result of our calculation is that periodate can react with $S_2O_3OH^-$ in two different pathways. The structure of $S_2O_3OH^-$ is supposed to be $HOSSO_3^-$, and attack of periodate on the sterically preferable S atom may be followed by scission of the S–S bond, leading to either sulfate and hypiodous acid (step 2) or HSO_3^- and iodate (step 3). This observation is not a unique feature of this species; in the chlorite–tetrathionate reaction, this effect was already observed and reported.¹² To strengthen the roles of k_2 and k_3 , additional fitting procedures have been carried out to indirectly support the necessity of these parallel steps. Eliminating them individually from the fitting procedure resulted not only in an unacceptably high increase of the average deviation (0.0106 and 0.0080, respectively) but also in a systematic deviation between the measured and calculated kinetic curves. Thus, we concluded that the role of these steps along with the given rate equations is confirmed.

Step 4, which eventually leads to the formation of tetrathionate, was already suggested by several independent research groups.^{22,23} It is found that the rate of this process is proportional to $[H^+]$, in agreement with the experimental findings that the formation of tetrathionate is preferred at lower pHs. We have also found that our value for k_4 is lower than that used by Schreiber et al.²³ in simulating the dynamical behavior of the tetrathionate–hydrogen peroxide reaction. In addition, we have not found any evidence that the rate equation of this reaction may have a pH-independent term under our experimental

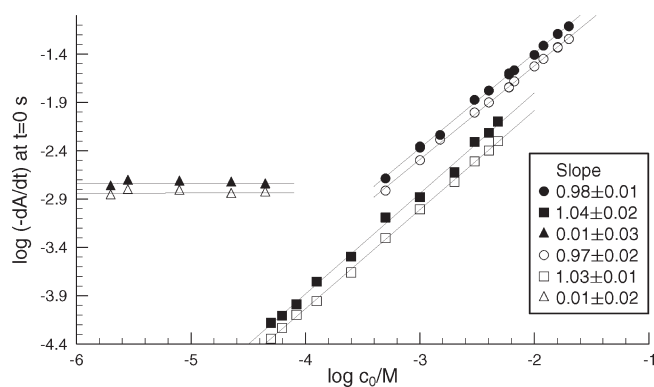


Figure 8. Initial rate studies at different conditions: $[IO_4^-]_0 = 2.00$ mM, pH = 5.55, and c_0 correspond to $[S_2O_3^{2-}]_0$ (●, ○); $[S_2O_3^{2-}]_0 = 0.50$ mM, pH = 5.55, and c_0 correspond to $[IO_4^-]_0$ (■, □); $[S_2O_3^{2-}]_0 = 0.50$ mM, $[IO_4^-]_0 = 2.00$ mM, and c_0 correspond to $[H^+]_0$ (▲, △). Filled and empty symbols belong to the measured kinetic curves at 275 and 290 nm, respectively.

conditions. Our calculation has revealed that k_4 can be calculated as $(7.7 \pm 0.2) \times 10^5 \text{ M}^{-2} \text{ s}^{-1}$ from our experiments. The role of this reaction is highly confirmed because this is the main route leading to the formation of tetrathionate.

Step 5 is the initiation of the thiosulfate–iodate reaction probably proceeding via an O-atom transfer from iodate to thiosulfate. As expected, we found that the rate of this reaction depends on $[H^+]$ but not on $[H^+]^2$, as was found by Rieder.²⁴ The fact that the rate of the overall thiosulfate–iodate reaction depends on $[H^+]^2$ has recently been explained²⁵ in terms of the rapid pH-dependent equilibrium formation of I_2O_2 from iodide and iodate ions and its subsequent reaction with thiosulfate. The fitting procedure also indicated that the rate coefficient of the back-reaction of step 5 can also be calculated from our experiments as $k_{-5} = (3.6 \pm 0.1) \times 10^7 \text{ M}^{-1} \text{ s}^{-1}$.

Step 6 is a comproportionation that produces iodate from the periodate ion and iodous acid via a simple O-atom transfer. The role of this reaction is to prevent the accumulation of iodous acid under those experimental conditions, where the concentration of the iodide ion is negligible. We also found this step to be pH-independent within the experimental conditions studied. The value of $k_6 = (2.1 \pm 0.1) \times 10^5 \text{ M}^{-1} \text{ s}^{-1}$ has worked consistently well in fitting the experimental traces, but it differs by a factor of 2 from that determined recently in the iodide–periodate reaction.²⁶ As we shall see later, this is not the only rate coefficient that works consistently well with values different from those reported previously. We have also tried to seek experimental evidence to explain these differences adequately. Figure 9 shows absorbance–time series measured at different buffer concentrations, keeping all of the other conditions unchanged. It clearly shows that the shape of the kinetic curves significantly changes with variation of the buffer concentration, meaning that at the later stages of the reaction strong buffer assistance must be involved in one or maybe more subsystems. This phenomenon frequently accompanies several reactions of oxyhalogen species.²⁷ Consequently, this means that the application of different buffer concentrations results in a notable difference in the determination of the value of the apparent rate coefficient of the given step.

Step 7 is the oxidation of hypiodous acid by the periodate ion to produce iodate and iodous acid. The rate coefficient of this

Table 1. Fitted and Fixed Rate Coefficients of the Proposed Kinetic Model^a

no.	chemical equation	rate equation	parameter
1	$\text{S}_2\text{O}_3^{2-} + \text{IO}_4^- + \text{H}^+ \rightleftharpoons \text{S}_2\text{O}_3\text{OH}^- + \text{IO}_3^-$	$k_1[\text{S}_2\text{O}_3^{2-}][\text{IO}_4^-]$ $k_{-1}[\text{S}_2\text{O}_3\text{OH}^-][\text{IO}_3^-]$	$k_1 = 7.36 \pm 0.07 \text{ M}^{-1} \text{ s}^{-1}$ $k_{-1} = 2.70 \pm 0.03 \text{ M}^{-1} \text{ s}^{-1}$
2	$\text{IO}_4^- + \text{S}_2\text{O}_3\text{OH}^- + \text{H}_2\text{O} \rightarrow \text{HOI} + 2\text{SO}_4^{2-} + 2\text{H}^+$	$k_2[\text{IO}_4^-][\text{S}_2\text{O}_3\text{OH}^-]$	$k_2 = 0.89 \pm 0.04 \text{ M}^{-1} \text{ s}^{-1}$
3	$\text{IO}_4^- + \text{S}_2\text{O}_3\text{OH}^- + \text{H}_2\text{O} \rightarrow 2\text{HSO}_3^- + \text{IO}_3^- + \text{H}^+$	$k_3[\text{IO}_4^-][\text{S}_2\text{O}_3\text{OH}^-]$	$k_3 = 1.50 \pm 0.03 \text{ M}^{-1} \text{ s}^{-1}$
4	$\text{S}_2\text{O}_3^{2-} + \text{S}_2\text{O}_3\text{OH}^- + \text{H}^+ \rightarrow \text{S}_4\text{O}_6^{2-} + \text{H}_2\text{O}$	$k_4[\text{H}^+][\text{S}_2\text{O}_3^{2-}][\text{S}_2\text{O}_3\text{OH}^-]$	$k_4 = (7.7 \pm 0.2) \times 10^5 \text{ M}^{-2} \text{ s}^{-1}$
5	$\text{S}_2\text{O}_3^{2-} + \text{IO}_3^- + 2\text{H}^+ \rightleftharpoons \text{S}_2\text{O}_3\text{OH}^- + \text{HIO}_2$	$k_5[\text{S}_2\text{O}_3^{2-}][\text{IO}_3^-][\text{H}^+]$ $k_{-5}[\text{S}_2\text{O}_3\text{OH}^-][\text{HIO}_2]$	$k_5 = (2.1 \pm 0.1) \times 10^5 \text{ M}^{-2} \text{ s}^{-1}$ $k_{-5} = (3.6 \pm 0.1) \times 10^7 \text{ M}^{-1} \text{ s}^{-1}$
6	$\text{IO}_4^- + \text{HIO}_2 \rightarrow 2\text{IO}_3^- + \text{H}^+$	$k_6[\text{IO}_4^-][\text{HIO}_2]$	$k_6 = (2.1 \pm 0.1) \times 10^5 \text{ M}^{-1} \text{ s}^{-1}$
7	$\text{IO}_4^- + \text{HOI} \rightarrow \text{IO}_3^- + \text{HIO}_2$	$k_7[\text{IO}_4^-][\text{HOI}]$	$k_7 = 39.2 \pm 1.5 \text{ M}^{-1} \text{ s}^{-1}$
8	$\text{IO}_4^- + \text{I}^- + \text{H}^+ \rightarrow \text{IO}_3^- + \text{HOI}$	$k_8[\text{IO}_4^-][\text{I}^-]$	$k_8 = 5.4 \pm 0.3 \text{ M}^{-1} \text{ s}^{-1}$
9	$\text{IO}_3^- + \text{I}^- + 2\text{H}^+ \rightleftharpoons \text{I}_2\text{O}_2 + \text{H}_2\text{O}$	$k_9[\text{IO}_3^-][\text{I}^-][\text{H}^+]^2$	$k_9 = (3.9 \pm 0.2) \times 10^8 \text{ M}^{-3} \text{ s}^{-1}$ $k_{-9} = 100 \text{ s}^{-1}$
10	$\text{I}_2 + \text{I}_2\text{O}_2 + 2\text{H}_2\text{O} \rightarrow 2\text{HIO}_2 + 2\text{I}^- + 2\text{H}^+$	$k_{10}[\text{I}_2][\text{I}_2\text{O}_2][\text{H}^+]$	$k_{10} = (9.2 \pm 1.1) \times 10^{10} \text{ M}^{-2} \text{ s}^{-1}$
11	$\text{HIO}_2 + \text{I}^- + \text{H}^+ \rightarrow 2\text{HOI}$	$k_{11}[\text{HIO}_2][\text{I}^-][\text{H}^+]$	$k_{11} = 10^9 \text{ M}^{-2} \text{ s}^{-1}$
12	$\text{I}_2 + \text{H}_2\text{O} \rightleftharpoons \text{HOI} + \text{I}^- + \text{H}^+$	$k_{12}[\text{I}_2]$ $k_{-12}[\text{HOI}][\text{I}^-][\text{H}^+]$	$k_{12} = 5.52 \times 10^{-2} \text{ s}^{-1}$ $k_{-12} = 1.02 \times 10^{11} \text{ M}^{-2} \text{ s}^{-1}$
13	$\text{I}_2 + \text{I}^- \rightleftharpoons \text{I}_3^-$	$k_{13}[\text{I}_2][\text{I}^-]$ $k_{-13}[\text{I}_3^-]$	$k_{13} = 5.6 \times 10^9 \text{ M}^{-1} \text{ s}^{-1}$ $k_{-13} = 8.5 \times 10^6 \text{ s}^{-1}$
14	$\text{HIO}_2 + \text{I}_2 + \text{H}_2\text{O} \rightarrow \text{IO}_3^- + 2\text{I}^- + 3\text{H}^+$	$k_{14}[\text{HIO}_2][\text{I}_2]$	$k_{14} = (1.4 \pm 0.1) \times 10^8 \text{ M}^{-1} \text{ s}^{-1}$
15	$\text{S}_2\text{O}_3^{2-} + \text{I}_2 \rightarrow \text{S}_2\text{O}_3\text{I}^- + \text{I}^-$	$k_{15}[\text{S}_2\text{O}_3^{2-}][\text{I}_2]$	$k_{15} = (2.0 \pm 0.1) \times 10^9 \text{ M}^{-1} \text{ s}^{-1}$
16	$\text{S}_2\text{O}_3\text{I}^- + \text{H}_2\text{O} \rightarrow \text{S}_2\text{O}_3^{2-} + \text{HOI} + \text{H}^+$	$k_{16}[\text{S}_2\text{O}_3\text{I}^-][\text{H}^+]$	$k_{16} = (2.4 \pm 0.2) \times 10^{11} \text{ M}^{-1} \text{ s}^{-1}$
17	$\text{IO}_4^- + \text{S}_2\text{O}_3\text{I}^- + 2\text{H}_2\text{O} \rightarrow 2\text{SO}_4^{2-} + \text{I}^- + \text{HOI} + 3\text{H}^+$	$k_{17}[\text{IO}_4^-][\text{S}_2\text{O}_3\text{I}^-]$	$k_{17} = (1.7 \pm 0.1) \times 10^6 \text{ M}^{-1} \text{ s}^{-1}$
18	$\text{S}_2\text{O}_3^{2-} + \text{HOI} \rightarrow \text{S}_2\text{O}_3\text{OH}^- + \text{I}^-$	$k_{18}[\text{S}_2\text{O}_3^{2-}][\text{HOI}][\text{H}^+]$	$k_{18} = (2.1 \pm 0.2) \times 10^7 \text{ M}^{-2} \text{ s}^{-1}$
19	$\text{S}_2\text{O}_3\text{OH}^- + \text{S}_2\text{O}_3\text{I}^- \rightarrow \text{S}_4\text{O}_6^{2-} + \text{HOI}$	$k_{19}[\text{S}_2\text{O}_3\text{OH}^-][\text{S}_2\text{O}_3\text{I}^-][\text{H}^+]$	$k_{19} = (4.7 \pm 0.2) \times 10^{12} \text{ M}^{-2} \text{ s}^{-1}$
20	$\text{HSO}_3^- + \text{I}_2 + \text{H}_2\text{O} \rightarrow \text{SO}_4^{2-} + 2\text{I}^- + 3\text{H}^+$	$k_{20}[\text{HSO}_3^-][\text{I}_2]$	$k_{20} = 3.1 \times 10^9 \text{ M}^{-1} \text{ s}^{-1}$
21	$\text{HSO}_3^- + \text{HOI} \rightarrow \text{SO}_4^{2-} + \text{I}^- + 2\text{H}^+$	$k_{21}[\text{HSO}_3^-][\text{HOI}]$	$k_{21} = 10^7 \text{ M}^{-1} \text{ s}^{-1}$
22	$\text{IO}_4^- + \text{HSO}_3^- \rightarrow \text{SO}_4^{2-} + \text{IO}_3^- + \text{H}^+$	$k_{22}[\text{IO}_4^-][\text{HSO}_3^-][\text{H}^+]$	$k_{22} = (1.6 \pm 0.1) \times 10^{10} \text{ M}^{-2} \text{ s}^{-1}$
23	$\text{S}_2\text{O}_3^{2-} + \text{HIO}_2 + \text{H}^+ \rightarrow \text{S}_2\text{O}_3\text{OH}^- + \text{HOI}$	$k_{23}[\text{S}_2\text{O}_3^{2-}][\text{HIO}_2][\text{H}^+]$	$k_{23} = (3.9 \pm 0.3) \times 10^{10} \text{ M}^{-2} \text{ s}^{-1}$
24	$2\text{S}_2\text{O}_3\text{OH}^- + \text{H}_2\text{O} \rightarrow \text{S}_2\text{O}_3^{2-} + 2\text{HSO}_3^- + 2\text{H}^+$	$k_{24}[\text{S}_2\text{O}_3\text{OH}^-]^2$	$k_{24} = 6.66 \pm 0.51 \text{ M}^{-1} \text{ s}^{-1}$
25	$\text{S}_2\text{O}_3\text{OH}^- + \text{IO}_3^- + \text{H}_2\text{O} \rightarrow 2\text{HSO}_3^- + \text{HIO}_2$	$k_{25}[\text{S}_2\text{O}_3\text{OH}^-][\text{IO}_3^-][\text{H}^+]$	$k_{25} = (2.2 \pm 0.2) \times 10^5 \text{ M}^{-2} \text{ s}^{-1}$
26	$\text{S}_4\text{O}_6^{2-} + \text{I}_2 \rightleftharpoons \text{S}_4\text{O}_6\text{I}^- + \text{I}^-$	$k_{26}[\text{S}_4\text{O}_6^{2-}][\text{I}_2]$ $k_{-26}[\text{S}_4\text{O}_6\text{I}^-][\text{I}^-]$	$k_{26} = 1.92 \text{ M}^{-1} \text{ s}^{-1}$ $k_{-26} = 10^7 \text{ M}^{-1} \text{ s}^{-1}$
27	$\text{S}_4\text{O}_6\text{I}^- + \text{H}_2\text{O} \rightarrow \text{S}_2\text{O}_3\text{OH}^- + \text{S}_2\text{O}_3\text{I}^- + \text{H}^+$	$k_{27}[\text{S}_4\text{O}_6\text{I}^-]$	$k_{27} = 214 \text{ s}^{-1}$
28	$\text{I}^- + \text{S}_4\text{O}_6\text{I}^- \rightarrow 2\text{S}_2\text{O}_3\text{I}^-$	$k_{28}[\text{I}^-][\text{S}_4\text{O}_6\text{I}^-]$	$k_{28} = 1.28 \times 10^5 \text{ M}^{-1} \text{ s}^{-1}$

^aNo error indicates that the value in question was fixed during the fitting procedure.

reaction was found to be $39.2 \pm 1.5 \text{ M}^{-1} \text{ s}^{-1}$, indicating that the oxidation of hypiodous acid by periodate is orders of magnitude slower than that of iodos acid. It also explains the fact that iodine can slowly be oxidized by periodate in an indirect way. The removal of iodine by periodate is, therefore, a consequence of the $\text{HOI}-\text{IO}_4^-$ reaction, followed by a shift in the well-known relatively rapid hydrolysis of iodine²⁸ in which HOI is involved (see later).

Step 8 is the well-known oxidation of iodide by the periodate ion. Present experiments indicate approximately half of the value of k_8 determined in previous independent studies^{26,29} but worked consistently during the fitting procedure here. These studies, however, also reported no *direct* buffer assistance in the iodide–periodate reaction, meaning that the apparent difference cannot be simply explained by this fact. However, as can be seen, the iodide ion is not an initial reactant in the present system; it is produced via a finite sequence of reactions. If the formation of the iodide ion is affected by the presence of buffer components and the absorbance–time series (which mainly corresponds to the

Table 2. Molar Absorbance (Given in $\text{M}^{-1} \text{ cm}^{-1}$ Units) of the Absorbing Species Used in the Fitting Procedure

λ (nm)	$\epsilon_{\text{S}_2\text{O}_3^{2-}}$	$\epsilon_{\text{IO}_4^-}$	$\epsilon_{\text{S}_4\text{O}_6^{2-}}$	$\epsilon_{\text{IO}_3^-}$	ϵ_{I^-}	ϵ_{I_2}	$\epsilon_{\text{I}_3^-}$
275	8.51	370.5	222.5	11.9	1.14	245.2	25055
280	4.54	317.1	158.4	5.95	0.87	260.6	32725
285	2.60	272.5	110.8	3.1	0.76	264.9	37605
290	1.64	231.9	75.5	1.76	0.70	251.5	38129
350	0	3.46	0	0	0	119.4	25489
400	0	0	0	0	0	241.8	6124
468	0	0	0	0	0	754.6	747.1

consumption of periodate) is at least partly determined by the iodide–periodate reaction, then one may observe a notable difference in the determination of the (apparent) rate coefficient of the given reaction. Certainly, this is a possible but not the only explanation of the experimental fact that we have found; consequently, more research is required to explore it more thoroughly.

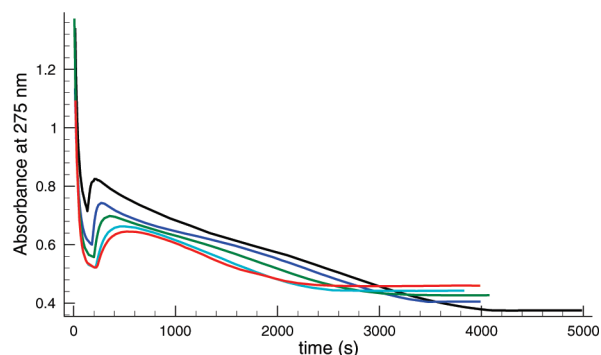


Figure 9. Measured absorbance–time curves at 275 nm with different buffer concentrations. Conditions: $[\text{S}_2\text{O}_3^{2-}]_0 = 3.68 \text{ mM}$, $[\text{IO}_4^-]_0 = 4.49 \text{ mM}$, $\text{pH} = 4.65$. The ionic strength is adjusted by sodium perchlorate to 0.5 M. $[\text{acetate}]_0/\text{M} = 0.5$ (black), 0.192 (blue), 0.1 (green), 0.042 (cyan), and 0.025 (red).

Step 9 is the well-known initiating step of the Dushman reaction³⁰ with the reversible formation of a short-lived intermediate I_2O_2 . We found that the absolute value of the forward rate coefficient (k_9) could be determined from our experiments, but the reverse one is in total correlation with k_{10} , which means that we, in fact, could calculate only the ratio k_{10}/k_{-9} . Our calculation has only provided a lower limit of 0.1 s^{-1} for k_{-9} . Because I_2O_2 is a short-lived intermediate, we set k_{-9} to 100 s^{-1} , which strictly fulfills this criterion, and calculated k_{10} . It is also interesting that no value is available for the forward and reverse rate coefficients of the initiating equilibrium of the Dushman reaction, although the rate coefficient of the global Dushman reaction was determined by several research groups. A good survey can be found in Schmitz's paper.²⁷ It is accepted that the rate equation of the Dushman reaction is given as $r = (4.2 \pm 0.8) \times 10^8 [\text{H}^+]^2 [\text{I}^-]^2 [\text{IO}_3^-]$ at $[\text{I}^-]_0 > 5 \times 10^{-6} \text{ M}$. Considering the reaction



and step 12 gives us the overall stoichiometry of the Dushman reaction. If I_2O_2 is treated as a short-lived steady-state intermediate with $k_{\text{I}} = 100 \text{ M}^{-1} \text{ s}^{-1}$, our measurements would provide a value of $(3.9 \pm 0.2) \times 10^8 \text{ M}^{-4} \text{ s}^{-1}$ for the overall rate coefficient of the Dushman reaction, which is in excellent agreement with the data reported by Schmitz.²⁷ Unfortunately, as can be seen below, the role of eq 6 is negligible under our experimental conditions, because eq 6 with a low iodide ion concentration is not able to compete with other reactions of I_2O_2 .

Step 10 is the only reaction of I_2O_2 that is necessary for a quantitative description of the measured absorbance–time series especially after Landolt time. As described above, the individual rate coefficient cannot be calculated because of the appearance of a total correlation between k_{10} and k_{-9} . We also found that the rate of this reaction is proportional to $[\text{H}^+]$ within the pH range studied. We have also tried to include the reaction of I_2O_2 by thiosulfate



and by the iodide ion (eq 6) with no success. The latter reaction was completely unnecessary, but inclusion of eq 7 resulted in a small change in the average deviation by less than 3%. Therefore, we concluded that eq 7 might play a significant role at different

experimental conditions (different initial concentrations, lower pH, etc.), but present experiments do not provide a solid basis to confirm its decisive contribution to the kinetics.

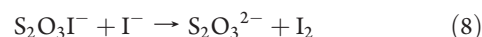
Step 11 is the well-known relatively fast comproportionation of iodosic acid and the iodide ion to produce hypoiodous acid. The rate coefficient of this process was fixed at $k_{11} = 10^9 \text{ M}^{-2} \text{ s}^{-1}$, as proposed by Lengyel and co-workers.³¹

Step 12, the well-known iodine hydrolysis, was already thoroughly studied by several research groups.²⁸ We adopted the forward and reverse rate coefficients determined by Lengyel et al.³¹

Step 13 is the rapid equilibrium formation of the triiodide ion investigated by several research groups independently.^{32,33} The rate coefficients of the forward and reverse reactions were set to $k_{13} = 5.7 \times 10^9 \text{ M}^{-1} \text{ s}^{-1}$ and $k_{-13} = 8.5 \times 10^6 \text{ s}^{-1}$, respectively, to give $\log \beta_{13} = 2.83$, where β_{13} is the formation constant of the triiodide ion.³⁴

Step 14 is the oxidation of iodosic acid by iodine to produce iodate and iodide ions. This reaction plays an important role at the later stages of the reaction. Omitting this step from the final model would result in not only a 0.0097 absorbance unit average deviation but also the appearance of a systematic deviation at those conditions, where iodine appears after Landolt time; therefore, its kinetic role was confirmed indirectly.

Step 15 is the initiating step of the well-known thiosulfate–iodine reaction.³⁵ Our calculation indicated that its rate coefficient has to be somewhat smaller [$k_{15} = (2.0 \pm 0.1) \times 10^9 \text{ M}^{-1} \text{ s}^{-1}$] than that of the corresponding hydrogen sulfite–iodine reaction. We also noticed a strong correlation between k_{15} and k_{20} ; therefore, our measurements provided enough information to determine only the ratio of k_{15}/k_{20} . Because k_{20} was reported by an independent study (see the discussion later), it allowed us to calculate the actual value of k_{15} as well. It should also be noted that inclusion of its back-reaction results in a small decrease in the average deviation by 2%. Although its role cannot be decisive in the overall kinetics,



the reaction may also be treated as a tentative step that may have a significant role at different experimental conditions. Therefore, we are inclined not to include it in the proposed model.

Step 16 is the pH-dependent hydrolysis of $\text{S}_2\text{O}_3\text{I}^-$ that produces thiosulfate and hypoiodous acid. Because $\text{S}_2\text{O}_3\text{I}^-$ was found to be a short-lived intermediate, one would expect that only the ratio of the rate coefficients of their further reactions could be calculated. Our calculations, however, resulted a clear minimum in the average deviation as a function of k_{16} , k_{17} , and k_{19} as well, from which we concluded that the absolute value of k_{16} as well as that of k_{17} and k_{19} could be determined. A possible explanation of this fact is that one of the reactants forms back through step 16, and the wide initial concentration range in $[\text{S}_2\text{O}_3^{2-}]_0$ carries enough experimental information for the simultaneous evaluation of the kinetic curves to calculate the absolute value of k_{16} . It is also interesting to note that this process is autocatalytic with respect to H^+ and plays a significant role in the first stage of the reaction, where the appropriate amount of HOI is produced.

Step 17 is the other manner of conversion of the short-lived intermediate $\text{S}_2\text{O}_3\text{I}^-$ that has a significant contribution at periodate excess, whereas step 16 has a greater influence at lower periodate concentrations. As pointed out before, because the

absolute value of k_{16} could be determined from the experiments, that of k_{17} could also be calculated.

Step 18 is the pH-dependent oxidation of thiosulfate by hypiodous acid probably proceeding via an O-atom transfer. This reaction prevents buildup of hypiodous acid in thio-sulfate excess. To strengthen the role of step 18 in the final model, we have also carried out an additional fitting procedure by eliminating k_{18} from the proposed model. The evaluation resulted in a significant increase of the average deviation (0.0263 absorbance unit) as well as in an appearance of the systematic deviation between the measured and calculated data. Therefore, we concluded that the role of step 18 is strongly confirmed.

Step 19 is another route to produce tetrathionate at lower pHs from $\text{S}_2\text{O}_3\text{OH}^-$ and $\text{S}_2\text{O}_3\text{I}^-$. The reason why the absolute value of k_{19} can be determined was already discussed previously. The role of this step was also confirmed by an additional fitting procedure, where k_{19} was omitted from the proposed model. The average deviation was increased unacceptably (0.0168 absorbance unit); therefore, its role is also highly established in the proposed model.

Step 20 is the well-known fast reaction between hydrogen sulfite and iodine, and its kinetics were thoroughly studied by Yiin and Margerum³⁶ and even the rate coefficient of this process was determined to be $3.1 \times 10^9 \text{ M}^{-1} \text{ s}^{-1}$. Therefore, we have fixed k_{20} at this value during the fitting process.

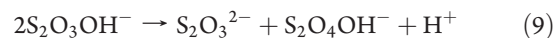
Step 21 is the rapid oxidation of hydrogen sulfite by hypiodous acid. Our calculation indicated that this reaction has to be fast to treat HSO_3^- as a steady-state intermediate. The actual rate coefficient cannot be determined from our experiments because there is a strong correlation between k_{21} and k_{22} . Any fixed value higher than $10^7 \text{ M}^{-1} \text{ s}^{-1}$ would result in the same average deviation; therefore, we decided to use the lower limit of the value for k_{21} .

Step 22 is the oxidation of hydrogen sulfite by the periodate ion via an O-atom transfer. We found that this reaction is pH-dependent and our calculation has provided a value of $(1.6 \pm 0.1) \times 10^{10} \text{ M}^{-2} \text{ s}^{-1}$ for k_{22} if k_{21} is fixed at $10^7 \text{ M}^{-1} \text{ s}^{-1}$, meaning that the ratio of $k_{22}/k_{21} = 1600 \pm 100 \text{ M}^{-1}$. This means that under our experimental conditions step 22 is a very rapid reaction and it cannot be studied by a conventional diode-array spectrophotometer. This point was strengthened by preliminary experiments indicating that the hydrogen sulfite–periodate reaction is, in fact, completed within less than a tenth of a second. Unfortunately, no research paper is available in the literature to provide independent information about the rate coefficient of this reaction that would also provide us a possibility to calculate the actual value of k_{21} .

Step 23 is the pH-dependent oxidation of thiosulfate by iodous acid, producing $\text{S}_2\text{O}_3\text{OH}^-$ and hypiodous acid, that probably proceeds via an O-atom transfer. As expected, it is a fast process that governs the reaction in the initial phase where a significant amount of thiosulfate is present. Omitting this reaction would lead to an increase of 0.0151 in the average deviation; therefore, we concluded that this step is also necessary for a quantitative description of the kinetic curves.

Step 24 is a second-order decomposition of $\text{S}_2\text{O}_3\text{OH}^-$, producing thiosulfate and hydrogen sulfite. We suggest that it probably proceeds through the following sequence of reactions (although any other alternative suggestion works

equivalently well):



where the rate-limiting process is eq 9. It is also interesting to note that the relatively low value of $k_{24} = 6.66 \pm 0.51 \text{ M}^{-1} \text{ s}^{-1}$ indicates that $\text{S}_2\text{O}_3\text{OH}^-$ is a long-lived intermediate of the reactions. This fact is not surprising at all because a significant role of $\text{S}_2\text{O}_3\text{OH}^-$ is already established in a different chemical system.²⁵ If this is true, one might also expect that in the UV range this species must have significant molar absorbance to contribute to the overall absorbance. As can be seen, the fitting procedure was executed in the wavelength range of 275–468 nm. Because we were able to achieve a sound quantitative agreement between the measured and calculated absorbances, it is concluded that within this range $\text{S}_2\text{O}_3\text{OH}^-$ does not have significant absorption. Probably at lower wavelengths, this conclusion is no longer valid, but under our experimental conditions, it is not necessary to include $\text{S}_2\text{O}_3\text{OH}^-$ in the final model as an absorbing species. The reason is simple because in this case the reactants already have enough absorbance contribution (especially the periodate ion) to the overall absorbance to exceed the 1.8 limit, where the linearity between the concentration and the measured signal is not fulfilled. That is why no fitting was executed below 275 nm. Of course, one might argue that lowering the initial concentration of the reactants allows us to calculate the molar absorbance of $\text{S}_2\text{O}_3\text{OH}^-$ from the kinetic curves but lowering the initial concentration would also result in a lower $\text{S}_2\text{O}_3\text{OH}^-$ concentration, meaning that its contribution to the overall absorbance becomes commensurable with the error of the absorbance measurements. Omitting this step from the model yields an average deviation of 0.0092 absorbance unit and systematic deviations between the measured and calculated kinetic curves; therefore, we concluded this reaction to be strongly confirmed.

Step 25 is the pH-dependent oxidation of the long-lived intermediate $\text{S}_2\text{O}_3\text{OH}^-$ by the iodate ion, producing hydrogen sulfite and iodous acid. We confirmed the role of this step indirectly by eliminating k_{25} from the final model. The simultaneous evaluation of the kinetic curves indicated a large increase in the average deviation (0.0104), from which we concluded that the role of this step is well-justified.

Steps 26–28 were directly adopted from our previous work without any change and fixed throughout the whole fitting procedure.¹⁴ It is clear that this set of reactions has a major influence on the later phase of the reaction after the Landolt time, where tetrathionate and iodine are present simultaneously. Under our experimental conditions, however, the amount of iodine formed is not significant ($T_{12} = [\text{I}_2] + [\text{I}_3^-] < 9 \times 10^{-5} \text{ M}$); therefore, we concluded that there is not enough experimental information to refine these parameters.

Finally, we shall point out how the complex absorbance–time profiles along with the changing stoichiometry can be understood by the proposed model. Figure 10 shows the measured absorbance–time profiles at 275 and 468 nm. At the beginning stage of the reaction, thiosulfate is oxidized simultaneously to tetrathionate and sulfate; meanwhile, periodate reduced to iodate, hypiodous acid, and the iodide ion. The concentration ratio of these species mainly depends on the pH and on the initial

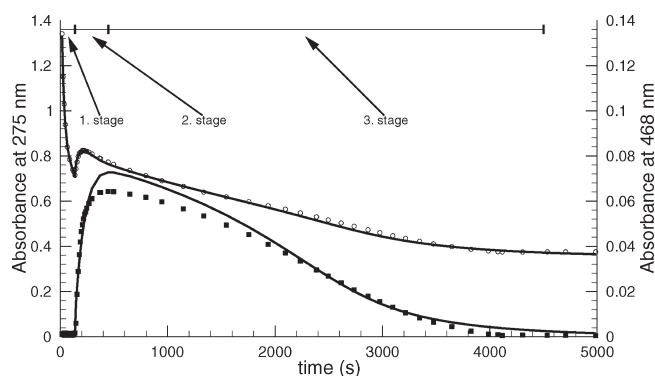


Figure 10. Three different stages of a complex absorbance–time curve. Conditions: $[\text{IO}_4^-]_0 = 4.90 \text{ mM}$; $[\text{S}_2\text{O}_3^{2-}]_0 = 3.68 \text{ mM}$; $\text{pH} = 4.65$. The left y axis belongs to symbols \circ , and the right y axis belongs to \blacksquare .

concentration ratio of the reactants. The net effect is that the absorbance steadily decreases at 275 nm. As long as the thiosulfate ion is present, iodine formed from step 12 is quickly removed to produce the iodide ion and hypoiodous acid through step 17. Eventually, this cycle increases the concentration of iodide and hypoiodous acid, and we shall see that the key species is hypoiodous acid in determining the kinetics of the following stage of the reaction. The first stage is finished when thiosulfate is completely removed from the solution. This time is usually defined as the Landolt time. Because iodine formed from step 12 is no longer consumed, it suddenly appears in the solution along with the triiodide ion. The amount of iodine is mainly determined by the amount of hypoiodous acid formed in the first stage of the reaction. This effect results in a sudden rise in absorbance at both 275 and 468 nm. Once hypoiodous acid is removed, the absorbance at 468 nm reaches its maximum. One may also notice that the maxima of the absorbance–time curves at 275 and 468 nm are shifted by approximately 200 s. This follows from the fact that the concentration of iodide is also decreased in the second stage, and as a result, the $\text{I}_2\text{--I}_3^-$ equilibrium is shifted toward the formation of iodine. Consequently, the amount of triiodide starts to decrease before all of hypoiodous acid is transformed to iodine. The third stage of the reaction starts after HOI is completely consumed. In this phase, the tetrathionate–iodine and iodide–periodate reactions slowly decrease the concentration of tetrathionate and periodate to produce sulfate and iodate. It is also interesting to note that the complex stoichiometry can also be understood via the proposed kinetic model. In high excess of periodate, steps 1, 2, 3, 6, 7, and 22 account for the stoichiometry given by eq 3, while in high excess of thiosulfate, steps 1, 4, 5, 18, and 23 completely explain the limiting stoichiometry given by eq 5. If the pH is higher and the excess of thiosulfate is moderate, then the net effect of steps 1, 9, 10, 11, 12, 20, 21, and 24 gives the stoichiometry characterized by eq 4. It should be emphasized, however, that these sequences of reactions cannot be separated experimentally; thus, it is quite difficult to reach each limiting stoichiometry, as noticed by Rábai et al.¹⁰

One might also argue that such a robust model can be described by almost any complex type of kinetic curve, and it is an overestimation of the number of kinetic parameters needed for an adequate description of the kinetic curves. To support the validity of our kinetic model, the following facts should be considered:

- A total of 18 steps of the proposed model have already been reported in previous studies. Either the majority of the rate coefficients were fixed to a known value during calculation or the values determined here were in sound agreement with the ones previously found. In some cases (such as steps 1, 9, and 22), no rate coefficient was available in the literature.
- The majority of the remaining steps are the reactions of periodate with different intermediates such as $\text{S}_2\text{O}_3\text{OH}^-$, $\text{S}_2\text{O}_3\text{I}^-$, and HSO_3^- , which are evidently necessary to prevent the accumulation of these species at high excess of periodate.
- Necessity of the newly proposed reactions such as steps 10, 14, 16, 18, 19, and 23 has been confirmed indirectly by the simultaneous evaluation of the kinetic curves. In each case, not only did the average deviation increased significantly but also the systematic deviation occurred between the measured and calculated kinetic data with the elimination of a given step.
- The proposed model also adequately explains the experimental fact that only small amounts of iodine can be accumulated during the reaction. This fact is due to the fine balance of iodide and hypoiodous acid formed during the Landolt time. For the appearance of iodine, the initial concentration ratio of the reactants has to be in a very narrow range. An increase of thiosulfate increases the amount of iodide but decreases that of hypoiodous acid, resulting in a cessation of the formation of iodine after a critical $[\text{S}_2\text{O}_3^{2-}]_0/[\text{IO}_4^-]_0$ ratio. In the opposite manner, an increase of periodate decreases the amount of iodide and leads to the exclusive formation of iodate.

It should also be mentioned that at first sight in the visible range the deviation between the measured and calculated data seems to be relatively large (see Figures 4 and S6G and S7G in the Supporting Information). It should be taken into consideration that in all of these cases the measured absorbance is relatively low and the average deviation of these kinetic curves is still around 0.006 absorbance unit, which is within the criterion of the acceptable fit defined in the Data Treatment section. Therefore, we concluded that the proposed model predicts the absorbance–time series at the visible range well within the error of the absorbance measurement. Further refinement of those parameters that are mainly responsible for the later phase of the reaction is only possible if the measured absorbance is enlarged approximately by an order of magnitude. As was seen previously, it is very difficult (if it is possible at all) to increase experimentally the amount of iodine to such an extent.

Finally, but not least, it has to be admitted that the proposed model in its present form is not able to explain all of the experimental findings (including the rare, fairly long transient period of damped oscillation) reported by Rábai et al.¹⁰ Further work is still underway in our laboratory to improve the model to be able to describe the most important dynamical feature of this system in a CSTR.

CONCLUSION

The work presented here may be considered as the first comprehensive effort to unravel the kinetics and mechanism of the complex thiosulfate–periodate reaction, although it is clear that we are only a step further in understanding the overall chemistry of this fascinating system. It is indubitably demonstrated that the initial phase of the reaction is completely

independent of the pH, and strong pH dependence can only be observed in the later phase of the reaction, where the role of the thiosulfate–periodate reaction is negligible. It is, therefore, expected that the rate law model of the thiosulfate–periodate reaction explaining the (oligo)oscillatory behavior in CSTR will further be refined in the near future for an adequate description of the experimental observations reported previously. It is demonstrated as well that strong buffer assistance plays a significant role in the later phase of the overall reaction. The present kinetic model, however, is not yet able to take this phenomenon into account but may pave the way for further investigations mainly focusing on the problems to be solved.

■ ASSOCIATED CONTENT

S Supporting Information. Listing of all of the chemical reactions taken into consideration prior to the start of the fit, presentation of the reproducibility of the kinetic curves, and additional measured and calculated kinetic curves. This material is available free of charge via the Internet at <http://pubs.acs.org>.

■ AUTHOR INFORMATION

Corresponding Author

*E-mail: horvatha@gamma.ttk.pte.hu.

■ ACKNOWLEDGMENT

This work was supported by Hungarian Research Fund Grant K68172. A.K.H. is grateful for the financial support of the János Bolyai Research Scholarship of the Hungarian Academy of Sciences.

■ REFERENCES

- (1) Field, R. J.; Burger, M., Eds. *Oscillations and Traveling Waves in Chemical Systems*, 1st ed.; Wiley-Interscience: London, 1985.
- (2) Ross, J.; Schreiber, I.; Vlad, M. O., Eds. *Determination of Complex Reaction Mechanisms*, 1st ed.; Oxford University Press: Oxford, U.K., 2005.
- (3) Belousov, B. P. *Ref. Radiats. Med.* 1958, *Medgiz, Moscow* 1959, 145.
- (4) Zhabotinsky, A. M. *Biofizika* 1964, 9, 306.
- (5) Bray, W. C. *J. Am. Chem. Soc.* 1921, 43, 1262–1267.
- (6) DeKepper, P.; Epstein, I. R.; Kustin, K.; Orbán, M. *J. Phys. Chem.* 1982, 86, 170–171.
- (7) (a) Rábai, G.; Beck, M. T. *J. Phys. Chem.* 1988, 92, 2804–2807. (b) Rábai, G.; Beck, M. T. *J. Phys. Chem.* 1988, 92, 4831–4835.
- (8) Nagypál, I.; Epstein, I. R. *J. Phys. Chem.* 1986, 90, 6285–6292.
- (9) Horváth, A. K. *J. Phys. Chem. A* 2008, 112, 3935–3942.
- (10) Rábai, G.; Beck, M. T.; Kustin, K.; Epstein, I. R. *J. Phys. Chem.* 1989, 93, 2853–2858.
- (11) Peintler, G.; Nagypál, I.; Epstein, I. R.; Kustin, K. *J. Phys. Chem. A* 2002, 105, 3899–3904.
- (12) Horváth, A. K.; Nagypál, I.; Epstein, I. R. *Inorg. Chem.* 2006, 45, 9877–9883.
- (13) Awtrey, A. D.; Connick, R. E. *J. Am. Chem. Soc.* 1951, 73, 4546–4549.
- (14) Kerek, A.; Horváth, A. K. *J. Phys. Chem. A* 2007, 111, 4235–4241.
- (15) Landolt, H. *Chem. Ber.* 1885, 18, 249.
- (16) Horváth, A. K.; Nagypál, I.; Peintler, G.; Epstein, I. R.; Kustin, K. *J. Phys. Chem. A* 2003, 107, 6966–6973.
- (17) Jenkin, M. E.; Sanders, S. M.; Pilling, M. J. *Atmos. Environ.* 1997, 31, 81–104.
- (18) Broadbelt, L. J.; Stark, S. M.; Klein, M. T. *Chem. Eng. Sci.* 1994, 49, 4991–5010.
- (19) Crouthamel, C. E.; Hayes, A. M.; Martin, D. S. *J. Am. Chem. Soc.* 1951, 73, 82–87.
- (20) Weavers, L. K.; Hua, L.; Hoffmann, M. R. *Water Environ. Res.* 1997, 69, 1112–1119.
- (21) Kustin, K.; Liebermann, E. C. *J. Phys. Chem.* 1964, 68, 3869–3873.
- (22) Kurin-Csörgei, K.; Orbán, M.; Rábai, G.; Epstein, I. R. *J. Chem. Soc., Faraday Trans.* 1996, 92, 2851–2855.
- (23) Voslar, M.; Matejka, P.; Schreiber, I. *Inorg. Chem.* 2006, 45, 2824–2834.
- (24) Rieder, R. *J. Phys. Chem.* 1930, 34, 2111–2116.
- (25) Varga, D.; Nagypál, I.; Horváth, A. K. *J. Phys. Chem. A* 2010, 114, 5752–5758.
- (26) Horváth, A. K. *J. Phys. Chem. A* 2007, 111, 890–896.
- (27) (a) Urbansky, E. T.; Cooper, B. T.; Margerum, D. W. *Inorg. Chem.* 1997, 36, 1338–1344. (b) Furman, C. S.; Margerum, D. W. *Inorg. Chem.* 1998, 37, 4321–4327. (c) Jia, Z. J.; Margerum, D. W.; Francisco, J. S. *Inorg. Chem.* 2000, 39, 2614–2620. (d) Schmitz, G. *Phys. Chem. Chem. Phys.* 1999, 1, 1909–1914. (e) Schmitz, G. *Phys. Chem. Chem. Phys.* 2000, 2, 4041–4044.
- (28) (a) Eigen, M.; Kustin, K. *J. Am. Chem. Soc.* 1962, 84, 1355–1361. (b) Palmer, D. A.; van Eldik, R. *Inorg. Chem.* 1986, 25, 928–931. (c) Lengyel, I.; Epstein, I. R.; Kustin, K. *Inorg. Chem.* 1993, 32, 5880–5882.
- (29) Marques, C.; Hasty, R. A. *J. Chem. Soc., Dalton Trans.* 1980, 111, 1269–1271.
- (30) Dushman, S. *J. Phys. Chem.* 1904, 8, 453–482.
- (31) Lengyel, I.; Li, J.; Kustin, K.; Epstein, I. R. *J. Am. Chem. Soc.* 1996, 118, 3708–3719.
- (32) Turner, D. H.; Flynn, G. W.; Sutin, N.; Beitz, J. V. *J. Am. Chem. Soc.* 1972, 94, 1554–1559.
- (33) Ruasse, M.; Aubard, J.; Galland, B.; Adenier, A. *J. Phys. Chem.* 1986, 90, 4382–4388.
- (34) *IUPAC Stability Constant Database*; Royal Society of Chemistry: London, 1992–1997.
- (35) Awtrey, A. D.; Connick, R. E. *J. Am. Chem. Soc.* 1951, 73, 1341–1348.
- (36) Yiin, B. S.; Margerum, D. W. *Inorg. Chem.* 1990, 29, 1559–1564.